

Multi-Orbital Molecular Compound (TTM-TTP)I₃: Effective Model and Fragment Decomposition

Masahisa TSUCHIIZU^{1*}, Yukiko OMORI¹, Yoshikazu SUZUMURA¹, Marie-Laure BONNET^{1,2†},
Vincent ROBERT^{2,3}, Shoji ISHIBASHI⁴, and Hitoshi SEO^{5,6}

¹Department of Physics, Nagoya University, Nagoya 464-8602, Japan

²Université de Lyon, Laboratoire de Chimie, Ecole Normale Supérieure de Lyon, CNRS, F-69364 Lyon, France

³Laboratoire de Chimie Quantique, UMR 7177 CNRS/Université de Strasbourg, F-67000 Strasbourg, France

⁴Nanosystem Research Institute (NRI) "RICS", AIST, Ibaraki 305-8568, Japan

⁵Condensed Matter Theory Laboratory, RIKEN, Wako, Saitama 351-0198, Japan

⁶JST, CREST, Wako, Saitama 351-0198, Japan

(Received December 27, 2010; J. Phys. Soc. Jpn. **80** (2011) 013703)

The electronic structure of the molecular compound (TTM-TTP)I₃, which exhibits a peculiar intra-molecular charge ordering, has been studied using multi-configuration *ab initio* calculations. First we derive an effective Hubbard-type model based on the molecular orbitals (MOs) of TTM-TTP; we set up a two-orbital Hamiltonian for the two MOs near the Fermi energy and determine its full parameters: the transfer integrals, the Coulomb and exchange interactions. The tight-binding band structure obtained from these transfer integrals is consistent with the result of the direct band calculation based on density functional theory. Then, by decomposing the frontier MOs into two parts, i.e., fragments, we find that the stacked TTM-TTP molecules can be described by a two-leg ladder model, while the inter-fragment Coulomb energies are scaled to the inverse of their distances. This result indicates that the fragment picture that we proposed earlier [M.-L. Bonnet *et al.*: J. Chem. Phys. **132** (2010) 214705] successfully describes the low-energy properties of this compound.

KEYWORDS: multi-orbital molecular compound, intra-molecular charge ordering, *ab initio* calculation, band calculation, fragment decomposition

A rich variety of physical properties have been explored in molecular solids since the realization of the first molecular metal, TTF-TCNQ, and in the last decade, charge-ordering (CO) phenomena and related issues have attracted much attention.^{1,2)} Despite the complexity of the constituent molecules, a simple picture works well for many compounds; the low-energy electronic properties are determined by a single frontier molecular orbital (MO). Therefore each molecule can be regarded as a single site, and then the tight-binding and Hubbard-type models based on this picture successfully describe their physical properties.^{2,3)} However, it has recently been recognized that such a simple single-MO approximation is not sufficient for describing the electronic structures of single-component molecular metals $M(\text{tmdt})_2$ [$M = \text{Ni}, \text{Au}$, etc.];^{4–6)} there are cases where multi-orbital effects reflecting the respective MOs induce unexpected novel physical properties.

In the present paper, we focus on a quasi-one-dimensional molecular crystal (TTM-TTP)I₃.^{7,8)} Since the formal charge of the TTM-TTP molecule is +1 owing to the monovalent counterion I₃[−], this compound was considered to be a half-filled system and the possibility of a genuine one-dimensional Mott insulator with paramagnetic spin properties was discussed.^{8–10)} However, it has also been pointed out that this system exhibits a transition toward a nonmagnetic state at around 80 K.^{11–13)} On the basis of detailed experimental analyses of this low-temperature phase by Raman scattering¹⁴⁾ and X-ray measurements,¹⁵⁾ a new type of CO state has been

proposed. This state is called the “intra-molecular CO” (ICO) state, where the inversion center on the middle point of the TTM-TTP molecule is lost and the charge is disproportionated *within* each molecule. This state cannot be described by the simple single-MO picture by its nature.

A key to understanding the electronic state of this compound, as shown in our previous theoretical work,¹⁶⁾ is that the singly-occupied-molecular-orbital (SOMO) and the second-highest-occupied-molecular-orbital (HOMO-1) of the ionic [TTM-TTP]⁺ molecule are close in energy. The chemical reason of this quasi-degeneracy can be understood in terms of a three-fragment model.¹⁶⁾ The SOMO and HOMO-1 are basically described by two of the fragments, as in the following. Since the TTM-TTP molecule itself has an inversion center, the resulting MOs can be classified into gerade (g) and ungerade (u) MOs. The SOMO (u MO) and HOMO-1 (g MO) are shown in Fig. 1, where the SOMO exhibits a bonding character between the left and right fragment MOs while the HOMO-1 has an antibonding character, i.e.,

$$\varphi_u \approx \frac{1}{\sqrt{2}}(\varphi_L + \varphi_R), \quad \varphi_g \approx \frac{1}{\sqrt{2}}(-\varphi_L + \varphi_R), \quad (1)$$

where φ_L and φ_R are the left (L) and right (R) fragment MOs.¹⁶⁾ The purpose of the present paper is to construct a minimal model that can describe the ICO state. The contribution of the center (C) fragment MO can be neglected for this purpose, since the C fragment is deep in energy.¹⁶⁾ We construct a two-orbital Hubbard-type model based on the SOMO and HOMO-1. The magnitudes of the intra-molecular and inter-molecular interactions are estimated from *ab initio* calculations with a complete-active-space configuration-

*E-mail: tsuchiiz@s.phys.nagoya-u.ac.jp

†Present address: Institute of Physical Chemistry, University of Zurich, Winterthurerstrasse 190, 8057 Zurich, Switzerland.

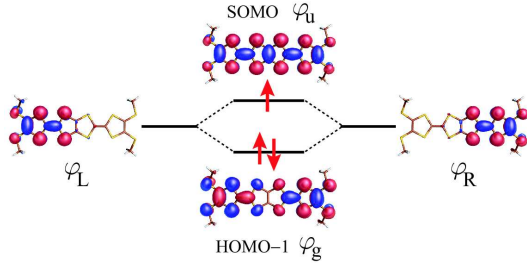


Fig. 1. (Color online) SOMO and HOMO-1 of the ionic $[\text{TTM-TTP}]^+$ molecule obtained by the restricted open-shell Hartree-Fock procedure,¹⁶ and a schematic energy diagram based on the left and right fragment MOs.

interaction (CAS-CI) method.¹⁷ By transforming the model into the fragment picture, we clarify that the stacked TTM-TTP molecules can be described by a two-leg ladder model.

The *ab initio* calculations were performed using the Molcas7 package¹⁷ with the basis set: S(7s6p1d)/[4s3p1d], C(5s5p1d)/[3s2p1d], and H(3s)/[1s]. The atomic parameters are taken from the results of the X-ray structure analysis at room temperature.⁷ As mentioned in ref. 16, the SOMO and HOMO-1 levels are well separated from the other MOs, and therefore, these two MOs are used to generate CAS[3,2] containing three electrons in two MOs. In order to evaluate the magnitudes of the inter-molecular interactions, we select two neighboring molecules and, in this case, put four MOs into the active space. Throughout the CI calculation, the MOs are fixed to the ones obtained from the restricted open-shell Hartree-Fock calculation.

First we derive the effective model Hamiltonian describing the isolated $[\text{TTM-TTP}]^+$ ion. In the CAS[3,2], there are two independent configurations: (i) one is the ungerade state g^2u^1 in which two electrons are on g and one electron is on u, and (ii) the other is the gerade state g^1u^2 with one electron on g and two electrons on u. In order to evaluate the Coulomb interactions, we also consider the configurations arising from the occupations of g and u MOs by 0, 1, 2 and 4 electrons. By the CAS-CI *ab initio* calculations, we can obtain the full energy spectrum and the information of the wave functions. By collecting these data, we can construct the two-orbital Hubbard-type Hamiltonian that reproduces the energy spectrum. Namely, we consider the following one-molecule Hamiltonian:

$$H_{1\text{-mol}} = E_0 + \varepsilon_g^0 n_g + \varepsilon_u^0 n_u + U_g n_{g,\uparrow} n_{g,\downarrow} + U_u n_{u,\uparrow} n_{u,\downarrow} + U' n_g n_u - J_H \left[\mathbf{S}_g \cdot \mathbf{S}_u - \frac{1}{2} (c_{g,\uparrow}^\dagger c_{g,\downarrow}^\dagger c_{u,\downarrow} c_{u,\uparrow} + \text{h.c.}) \right], \quad (2)$$

where $c_{g,\sigma}$ ($c_{u,\sigma}$) is the electron annihilation operator for g (u) MO of the TTM-TTP molecule. The quantities ε_g^0 and ε_u^0 represent the energy levels of the g and u MOs. U_g (U_u) represents the Coulomb repulsion between two electrons on the g (u) MO, and U' is the inter-MO Coulomb repulsion. J_H is the Hund coupling including the pair-hopping term, and E_0 is the energy constant. In contrast with the case of atomic orbitals under the centrosymmetric potential, there is no constraint relation among these couplings. The density operators are nor-

Table I. Estimated parameters for the isolated TTM-TTP molecule.

Energy level	Intra-orbital interaction	Inter-orbital interaction
$\varepsilon_g^0 = -8.63$ eV	$U_g = 3.70$ eV	$U' = 2.82$ eV
$\varepsilon_u^0 = -8.21$ eV	$U_u = 3.90$ eV	$J_H = 3.19$ eV

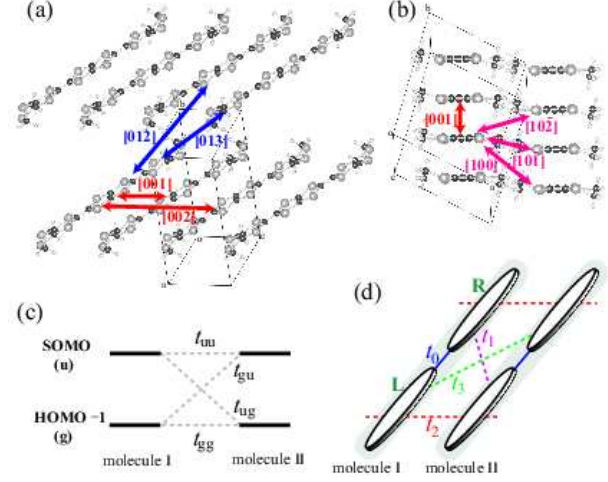


Fig. 2. (Color online) Crystal structure of the $(\text{TTM-TTP})\text{I}_3$ projected onto the b - c plane (a) and onto the a - c plane (b). Definitions of transfer integrals in the MO basis (c) and in the fragment basis (d).

mal ordered, i.e., $n_{\nu,\sigma} = (c_{\nu,\sigma}^\dagger c_{\nu,\sigma} - 3/4)$ with $\nu = g, u$. Here, we note that the charges on each MO are set as $3/4$ in order to treat the g and u MOs on the same footing.¹⁶ The evaluated parameters are summarized in Table I. The energy level difference between u and g MOs is relatively small, ≈ 0.42 eV, which reproduces the results reported in ref. 16. The magnitudes of U_g and U_u are small compared with those of smaller molecules such as the TTF molecule in TTF-TCNQ, for which we obtained $U_{\text{TTF}} \approx 6.2$ eV. In addition, U_u is slightly larger than U_g , a reflection of the left-right bonding character of the u MO compared with the antibonding character of the g MO. The Coulomb repulsion for the TTF molecule was estimated from the density-functional-theory calculations to be ≈ 4.7 eV,¹⁸ which is comparable to our result. As a reference, we note that the magnitude of the bare Coulomb repulsion of the BEDT-TTF dimer in the κ -(BEDT-TTF)₂X system is about 3 - 4 eV.^{19,20} We also note that relatively large Hund coupling is obtained ($J_H/U_u \approx 0.8$), in contrast to those for transition-metal atoms.

Next we evaluate the inter-molecular interactions. We focus on two neighboring TTM-TTP molecules whose atomic coordinates are read from the crystal structure at room temperature, and perform CAS-CI calculations using the MOs for the isolated $[\text{TTM-TTP}]^+$ molecule. In order to determine this set of MOs, the two molecules were artificially displaced with respect to one another so that the intermolecular overlap was negligible. Hereafter, we refer to the two target molecules as “molecule I” and “molecule II”. The molecule pairs that we have focused on are shown in Figs. 2(a) and 2(b). The Hamiltonian for one-body terms that appear in the two-molecule

system is given by

$$H'_{2\text{-mol}} = -t_{gg}c_{g,I,\sigma}^\dagger c_{g,II,\sigma} - t_{uu}c_{u,I,\sigma}^\dagger c_{u,II,\sigma} - t_{gu}c_{g,I,\sigma}^\dagger c_{u,II,\sigma} - t_{ug}c_{u,I,\sigma}^\dagger c_{g,II,\sigma} + \text{h.c.} + \Delta\varepsilon_g(n_{g,I} + n_{g,II}) + \Delta\varepsilon_u(n_{u,I} + n_{u,II}) + H'_\Delta, \quad (3)$$

where the parameters t_{gg} and t_{uu} are the inter-molecular transfer integrals for the same g and u MOs, respectively, while t_{gu} and t_{ug} are for different MOs [see Fig. 2(c)]. The summation over repeated spin indices is implied. In terms of the *ab initio* Hamiltonian H , these transfer integrals are expressed as $t_{gg} \equiv -\langle\varphi_{g,I}|H|\varphi_{g,II}\rangle$, $t_{uu} \equiv -\langle\varphi_{u,I}|H|\varphi_{u,II}\rangle$, and $t_{gu} \equiv -\langle\varphi_{g,I}|H|\varphi_{u,II}\rangle = +\langle\varphi_{u,I}|H|\varphi_{g,II}\rangle = -t_{ug}$, where $|\varphi_{g,I}\rangle$ ($|\varphi_{g,II}\rangle$) and $|\varphi_{u,I}\rangle$ ($|\varphi_{u,II}\rangle$) are the states with a single electron on the g MO and u MO in molecule I (II), respectively. The parameters $\Delta\varepsilon_g$ and $\Delta\varepsilon_u$ represent the energy-level shift due to the potential energy from the other molecule. The additional term is $H'_\Delta = \Delta\varepsilon_{gu}(c_{g,I,\sigma}^\dagger c_{u,I,\sigma} - c_{g,II,\sigma}^\dagger c_{u,II,\sigma} + \text{h.c.})$, which reflects the asymmetry between L/R fragments within the molecule and disappears when one considers the periodic crystal system. The possible inter-molecular Coulomb interaction terms are represented as

$$H''_{2\text{-mol}} = V_{gg}n_{g,I}n_{g,II} + V_{uu}n_{u,I}n_{u,II} + V_{gu}(n_{g,I}n_{u,II} + n_{u,I}n_{g,II}) + \left[I(c_{g,I,\sigma}^\dagger c_{u,I,\sigma} c_{u,II,\sigma'}^\dagger c_{g,II,\sigma'} + c_{g,I,\sigma}^\dagger c_{u,I,\sigma} c_{g,II,\sigma'}^\dagger c_{u,II,\sigma'}) + X_g(n_{g,I}c_{g,II,\sigma}^\dagger c_{u,II,\sigma} - c_{g,I,\sigma}^\dagger c_{u,I,\sigma} n_{g,II}) + X_u(n_{u,I}c_{g,II,\sigma}^\dagger c_{u,II,\sigma} - c_{g,I,\sigma}^\dagger c_{u,I,\sigma} n_{u,II}) + \text{h.c.} \right], \quad (4)$$

where V_{gg} (V_{uu}) and V_{gu} denote the inter-molecular density-density interactions on the same g (u) MOs and between the g and u MOs, respectively. The I term represents the orbital exchange interaction and the X_g and X_u terms are the density-hopping interactions. As in the case of the isolated molecule, we can determine the parameters in eqs. (3) and (4) by using the *ab initio* energies for states with different symmetry, spin states, and electron numbers. The evaluated parameters are summarized in Table II. In contrast to the conventional extended Hückel approach, where the overlap integrals are used in the band calculation,²¹⁾ we can directly obtain the transfer integrals along different directions $[ijk]$ in the present approach. We find that only the nearest-neighbor transfer integrals along the stacking [001] direction are large

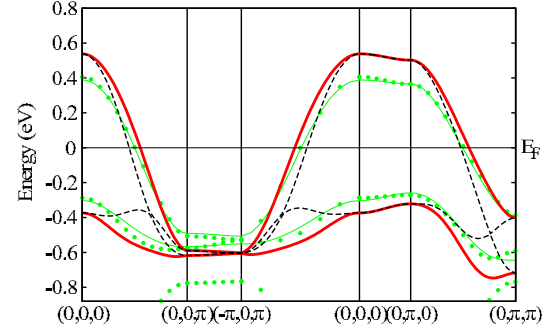


Fig. 3. (Color online) Band structure of (TTM-TTP) I_3 obtained from the tight-binding parameters evaluated by the CAS-CI *ab initio* calculations (thick solid red lines). The dashed lines represent the energy dispersion in the case of $t_{gu} = 0$. The GGA and its fitted results are shown by green dots and thin solid green lines, respectively.

and the magnitude of $t_{uu}^{[001]}$ becomes comparable to the value estimated by the extended Hückel approach (≈ 0.26 eV).⁷⁾ We also note that the energy-level shifts are relatively large, e.g., for the [001] molecule pair, we find $\Delta\varepsilon_g^{[001]} = -1.81$ eV and $\Delta\varepsilon_u^{[001]} = -1.85$ eV. The magnitudes of the inter-molecular density-density repulsions are relatively large compared with the intra-molecular interaction ($V_{gg}/U_g \approx 0.57$ and $V_{uu}/U_u \approx 0.59$), whereas a similar value is also obtained in the benchmark TTF chain in TTF-TCNQ as $V/U \approx 0.52$.

On the basis of the results of the above analysis, we examine the band structure of the (TTM-TTP) I_3 crystal in the metallic state. By neglecting correlation effects, the band structure obtained from the crystal version of eq. (3) is shown in Fig. 3. Here, we assign the energy levels for each MO as $\varepsilon_g = \varepsilon_g^0 + 2\Delta\varepsilon_g^{[001]} = -12.25$ eV and $\varepsilon_u = \varepsilon_u^0 + 2\Delta\varepsilon_u^{[001]} = -11.90$ eV. However, these absolute values should be refined by taking into account other molecules as well as counterion I_3^- . For comparison, electronic-structure calculations were carried out directly for the (TTM-TTP) I_3 crystal with the computational code QMAS (Quantum Materials Simulator)²²⁾ based on the generalized gradient approximation (GGA).²³⁾ The resulting band structure is shown in Fig. 3. Despite the bandwidth being overestimated owing to the neglect of correlation effects, the overall band structure obtained from eq. (3) agrees with the GGA results, indicating the validity of the present approach based on the CAS-CI *ab initio* calculations. The hypothetical band structure obtained by neglecting the SOMO–HOMO-1 mixing (i.e., we set $t_{gu} = 0$) is also shown by the dashed lines in Fig. 3. We find that the SOMO band has large dispersion along the [001] direction, whereas the HOMO-1 band is very narrow and is located within the SOMO band. Furthermore, these two bands are isolated and thus we can conclude that this system can be regarded as a two-band system.

Finally we transform the model into the fragment picture by using eq. (1), where the stacked TTM-TTP molecules can be described as an effective two-leg ladder system, as shown in Fig. 2(d). The transfer integral between the L and R fragments within the molecule is characterized by the energy difference between the g and u MOs, i.e., $t_0 = (\varepsilon_g - \varepsilon_u)/2 \approx -0.17$ eV. The Coulomb interaction within the fragment, i.e., the

Table II. Estimated parameters for the inter-molecular interactions in the MO picture. All energies are in eV.

	[001]	[002]	[012]	[013]	[100]	[101]	[102]
t_{gg}	-0.04	0.00	0.03	-0.02	0.00	0.01	0.00
t_{uu}	-0.29	0.00	-0.02	0.01	0.00	0.00	0.00
t_{gu}	-0.13	0.00	-0.02	0.01	0.00	0.00	0.00
V_{gg}	2.12	1.30	1.17	0.89	1.20	1.13	0.90
V_{uu}	2.30	1.30	1.09	0.83	1.24	1.12	0.87
V_{gu}	2.21	1.31	1.13	0.85	1.22	1.13	0.89
I	0.26	-0.03	-0.14	-0.09	0.06	-0.05	-0.06
X_g	-0.27	-0.26	-0.31	-0.22	0.13	0.22	0.18
X_u	-0.45	-0.29	-0.29	-0.20	0.17	0.23	0.18

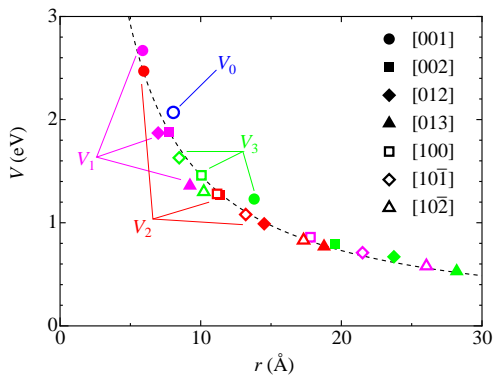


Fig. 4. (Color online) Distance dependence of the inter-fragment Coulomb repulsions. The dotted line represents the bare Coulomb repulsion. The Coulomb repulsion within the fragment is $U = 5.30$ eV.

“on-site” repulsion, is $U = 5.30$ eV, which becomes comparable to that for the TTF molecule, $U_{\text{TTF}} \approx 6.2$ eV, while the Coulomb and exchange interactions between the L and R fragments are $V_0 = 2.07$ eV and $J = 0.18$ eV. Let us stress that J_H is not directly reduced to the exchange coupling between the L and R moieties. For the inter-molecular interactions, there are three kinds of transfer integrals, t_1 , t_2 , and t_3 [shown in Fig. 2(d)], and corresponding Coulomb repulsions, V_1 , V_2 , and V_3 . The correspondence relations between the transfer integrals in the MO basis and those in the fragment basis are given by $t_1 = (-t_{gg} + t_{uu} + 2t_{gu})/2$, $t_2 = (t_{gg} + t_{uu})/2$, and $t_3 = (-t_{gg} + t_{uu} - 2t_{gu})/2$. The dominant transfer integrals (> 0.01 eV) are $t_0 = -0.17$, $t_1^{[001]} = -0.26$, $t_2^{[001]} = -0.17$, $t_1^{[012]} = -0.05$, and $t_1^{[013]} = 0.02$, where all energies are given in eV. By fitting the GGA band calculation, these are estimated as $t_0 = -0.12$, $t_1^{[001]} = -0.20$, $t_2^{[001]} = -0.14$, $t_1^{[012]} = -0.03$, and $t_1^{[013]} = 0.01$. The fitted band structure is shown by the thin solid lines in Fig. 3. We obtain qualitatively consistent parameters, and it is worth noting that the inter-fragment transfer integral within the molecule $|t_0|$ is smaller than the inter-molecular transfer integral $|t_1^{[001]}|$. A similar situation has been pointed out in single-component molecular metals.⁶⁾

We have also calculated the Coulomb repulsions as a function of distance between the fragments. We define the inverse of the inter-fragment distance, $1/r$, as the average inverse distance between 6 sulfur atoms in each fragment. The magnitudes of interactions follow surprisingly well the $1/r$ Coulomb law, including the intra-molecular interaction V_0 , as shown in Fig. 4. This result strongly supports our fragment decomposition picture. In conventional single-orbital compounds, the bare Coulomb interactions are known to follow the Coulomb law as a function of the inter-molecular distance.^{19,24)} In addition, we find that the inter-fragment distance for the [001] interactions becomes shorter than that for the intra-molecular one, and then the interactions $V_1^{[001]}$ and $V_2^{[001]}$ exceed the intra-molecular interaction V_0 . This feature would be a key ingredient in obtaining the intra-molecular degree of freedom, and particularly for the ICO phenomena. However, we should note that the screening effects in the crystal are not taken into account. Such effects have been examined in the single-orbital system,^{18,19)} and it remains future

work to extend the analysis to the multi-orbital systems.

We briefly discuss the electronic states in (TTM-TTP) I_3 on the basis of the present fragment-MO picture. From the simple “atomic” limit analysis of our model, where the kinetic energy is neglected, we indeed find that the lowest-energy state is the ICO state in which the charge is disproportionated at the R (L) fragment in molecule I (II) in Fig. 2(d). This ICO pattern is compatible with the $q = (0, 0, 1/2)$ superstructure observed by the X-ray measurements.^{11,12,15)} On the basis of this finding, we infer that the non-magnetic insulating behavior observed at low temperatures^{11–13)} is attributed to the spin-singlet formation on the $t_1^{[001]}$ bond with two-fold periodicity along the stacking direction. On the other hand, the paramagnetic non-metallic state seen at high temperature^{7–9)} might be due to the charge localization on each $t_1^{[001]}$ bond, since $t_1^{[001]}$ is the strongest bond in the system. A detailed analysis of possible ordered states based on the derived effective model will be published elsewhere.

In summary, we have constructed an effective Hubbard-type Hamiltonian and examined the electronic band structure for the multi-orbital molecular compound (TTM-TTP) I_3 . It has been clarified that the present scheme combined with the *ab initio* calculations is consistent with the GGA calculation. We have found that, in the fragment picture, the stacked TTM-TTP molecules can be described by the effective two-leg ladder and the Coulomb repulsions are proportional to the inverse of the inter-fragment distance.

Acknowledgements

MT thanks S. Yasuzuka, T. Kawamoto, T. Mori, and K. Yakushi for fruitful discussions on the experimental aspects of (TTM-TTP) I_3 . MT and YO also thank L. Cano-Cortés, J. Merino, and K. Nakamura for discussions on the parameter evaluations of the molecular solids. YO and MLB were supported by the Grant-in-Aid for JSPS Fellows. This research was partially supported by Grants-in-Aid for Scientific Research on Innovative Areas (20110002, 20110003, and 20110004) from the Ministry of Education, Culture, Sports, Science and Technology, Japan.

- 1) T. Mori: Chem. Rev. **104** (2004) 4947.
- 2) H. Seo, C. Hotta, and H. Fukuyama: Chem. Rev. **104** (2004) 5005.
- 3) H. Seo, J. Merino, H. Yoshioka, and M. Ogata: J. Phys. Soc. Jpn. **75** (2006) 051009.
- 4) H. Tanaka, Y. Okano, H. Kobayashi, W. Suzuki, and A. Kobayashi: Science **291** (2001) 285.
- 5) C. Rovira, J. J. Novoa, J.-L. Mozos, P. Ordejón, and E. Canadell: Phys. Rev. B **65** (2002) 081104.
- 6) S. Ishibashi, H. Tanaka, M. Kohyama, M. Tokumoto, A. Kobayashi, H. Kobayashi, and K. Terakura: J. Phys. Soc. Jpn. **74** (2005) 843; S. Ishibashi, K. Terakura, and A. Kobayashi: J. Phys. Soc. Jpn. **77** (2008) 024702; H. Seo, S. Ishibashi, Y. Okano, H. Kobayashi, A. Kobayashi, H. Fukuyama, and K. Terakura: J. Phys. Soc. Jpn. **77** (2008) 023714.
- 7) T. Mori, H. Inokuchi, Y. Misaki, T. Yamabe, H. Mori, and S. Tanaka: Bull. Chem. Soc. Jpn. **67** (1994) 661.
- 8) T. Mori, T. Kawamoto, J. Yamaura, T. Enoki, Y. Misaki, T. Yamabe, H. Mori, and S. Tanaka: Phys. Rev. Lett. **79** (1997) 1702.
- 9) S. Yasuzuka, K. Murata, T. Fujimoto, M. Shimotori, T. Kawamoto, T. Mori, H. Masato, and Y. Uwatoko: J. Phys. Soc. Jpn. **75** (2006) 053701.
- 10) M. Tsuchiizu, Y. Suzumura, and C. Bourbonnais: Phys. Rev. Lett. **99** (2007) 126404.
- 11) M. Maesato, Y. Sasou, S. Kagoshima, T. Mori, T. Kawamoto, Y. Misaki, and T. Yamabe: Synth. Met. **103** (1999) 2109.

- 12) N. Fujimura, A. Namba, T. Kambe, Y. Nogami, K. Oshima, T. Mori, T. Kawamoto, Y. Misaki, and T. Yamabe: *Synth. Met.* **103** (1999) 2111.
- 13) M. Onuki, K. Hiraki, T. Takahashi, D. Jinno, T. Kawamoto, T. Mori, T. Takano, and Y. Misaki: *Synth. Met.* **120** (2001) 921; M. Onuki, K. Hiraki, T. Takahashi, D. Jinno, T. Kawamoto, T. Mori, K. Tanaka, and Y. Misaki: *J. Phys. Chem. Solids* **62** (2001) 405.
- 14) K. Yakushi, R. Świetlik, K. Yamamoto, T. Kawamoto, T. Mori, Y. Misaki, and K. Tanaka: *Synth. Met.* **135** (2003) 583; R. Świetlik, K. Yakushi, K. Yamamoto, T. Kawamoto, and T. Mori: *J. Mol. Str.* **704** (2004) 89; R. Świetlik, K. Yakushi, K. Yamamoto, T. Kawamoto, and T. Mori: *Synth. Met.* **150** (2005) 83.
- 15) Y. Nogami, T. Kambe, N. Fujimura, K. Oshima, T. Mori, and T. Kawamoto: *Synth. Met.* **135-136** (2003) 637.
- 16) M.-L. Bonnet, V. Robert, M. Tsuchiizu, Y. Otori, and Y. Suzumura: *J. Chem. Phys.* **132** (2010) 214705.
- 17) G. Karlström, R. Lindh, P.-Å. Malmqvist, B.O. Roos, U. Ryde, V. Veryazov, P.-O. Widmark, M. Cossi, B. Schimmelpfennig, P. Neogrady, and L. Seijo: *Comp. Mater. Sci.* **28** (2003) 222.
- 18) L. Cano-Cortés, A. Dolfen, J. Merino, J. Behler, B. Delley, K. Reuter, and E. Koch: *Eur. Phys. J. B* **56** (2007) 173.
- 19) K. Nakamura, Y. Yoshimoto, T. Kosugi, R. Arita, and M. Imada: *J. Phys. Soc. Jpn.* **78** (2009) 083710.
- 20) E. Scriven and B. J. Powell: *J. Chem. Phys.* **130** (2009) 104508; *Phys. Rev. B* **80** (2009) 205107.
- 21) T. Mori, A. Kobayashi, Y. Sasaki, H. Kobayashi, G. Saito, and H. Inokuchi: *Bull. Chem. Soc. Jpn.* **57** (1984) 627.
- 22) S. Ishibashi, T. Tamura, S. Tanaka, M. Kohyama, and K. Terakura: <http://www.qmas.jp>.
- 23) J. P. Perdew, K. Burke, and M. Ernzerhof: *Phys. Rev. Lett.* **77** (1996) 3865.
- 24) T. Mori: *Bull. Chem. Soc. Jpn.* **73** (2000) 2243.